Resource Allocation of Terrestrial-Satellite Service in Coexistence with Earth Exploration Satellites

Kai-Tse Wu, Po-Chen Wu, Li-Hsiang Shen*, Kai-Ten Feng, Zhi Ding†, Jen-Ming Wu‡
Department of Electronics and Electrical Engineering, National Yang Ming Chiao Tung University, Hsinchu, Taiwan
*Department of Communication Engineering, National Central University, Taoyuan, Taiwan
†Department of Electrical and Computer Engineering, University of California, Davis, CA, USA
‡Next-generation Communications Research Center, Hon Hai Research Institute, Taipei, Taiwan
Email: {morris0112.ee12, wupochen.ee11}@nycu.edu.tw, shen@ncu.edu.tw,
ktfeng@nycu.edu.tw, zding@ucdavis.edu, jen-ming.wu@foxconn.com

***Abstract*—Earth exploration satellite service (EESS) plays a crucial role in environmental monitoring and weather forecasting by utilizing passive sensing technologies. However, the rapid expansion of terrestrial and satellite communication networks has introduced significant interference challenges, particularly in frequency bands that overlap with or are adjacent to EESS sensors. In this work, we develop a system model that explicitly characterizes EESS interference by considering reflected signal effects and spatial interference accumulation. Based on this model, we propose a EESS-aware resource allocation (EARA) framework that jointly optimizes power allocation and user association, while ensuring that interference to EESS sensors remains within acceptable limits. A non-convex joint optimization problem is formulated and efficiently solved leveraging the Lagrangian dual transform and Dinkelbach's method. Simulation results demonstrate that the proposed EARA scheme achieves up to 26.3% higher sum rate compared to genetic algorithm and binary whale optimization algorithm, while strictly satisfying the ITU-defined interference threshold. This work establishes a foundation for future research on the coexistence of communication networks and passive Earth observation systems, offering practical strategies for interference mitigation and spectrum sharing in next-generation networks.**

***Index Terms*—Earth exploration satellite, LEO satellites, terrestrial networks, resource allocation, mixed-integer optimization.**

I. Introduction

The Earth exploration satellite service (EESS) is a program that consists of a series of satellites, sensors, and ground-based systems designed to monitor the Earth's atmosphere, land, and oceans [1]. The primary goal of EESS is to provide scientists, researchers, and decision-makers with real-time data on weather patterns, and environmental changes. Passive remote sensing technologies play a pivotal role in EESS by detecting natural radiation emitted or reflected from the Earth's surface without actively emitting signals. These sensors are critical for weather forecasting and environmental monitoring by measuring key atmospheric parameters, such as water vapor [2]. However, the effectiveness of such sensors is increasingly threatened by interference from emerging wireless networks operating in adjacent frequency bands.

Recent research shows that signals from wireless networks can overlap with the frequencies used by passive sensors [3], [4]. Such interference reduces its accuracy and may lead to errors in weather predictions or environmental monitoring. Paper [5] examines the interference between 5G mm-wave networks and weather satellites operating in the 23.8 GHz band. The findings indicate that the cumulative interference from an entire network, particularly in urban areas, could exceed acceptable limits for satellite passive sensing. The authors in [6] models the interference between 6G networks and passive sensing systems. In [7], the authors study spectrum sharing above 100 GHz, addressing interference to Earth observation satellites via band switching. Nevertheless, the above-mentioned studies only focus on channel modeling and radio frequency interference (RFI) analysis. They do not address how, in real-world scenarios, radio resources can be intelligently allocated to minimize interference to EESS satellites.

While existing studies have primarily focused on mitigating interference in passive sensing systems, research on intelligent resource allocation to minimize such interference remains limited. Most prior work has instead explored various aspects of communication performance and resource management in terrestrial networks. For instance, [8] addresses resource allocation challenges in multiple terrestrial base station (TBS) orthogonal frequency division multiplexing (OFDM) systems under high-speed scenarios. In [9], the authors address energy-efficient resource allocation in OFDM access (OFDMA) networks with massive TBS antennas, aiming to optimize the energy efficiency (EE) of TBS operations. However, these solutions are designed for terrestrial networks and do not account for the unique constraints of satellite-based sensing systems like EESS. To overcome the coverage limitations of TBS networks, low Earth orbit (LEO) satellite systems have emerged as a promising solution for providing global and seamless communication services.

In [10], the authors propose a hierarchical multi-agent framework for dynamic power, beam, and channel allocation in multi-LEO satellite systems. Similarly, [12] focuses on enhancing EE and beam alignment accuracy while reducing latency, optimizing on power allocation and beam resource management. While TBS excels in delivering high-capacity, low-latency communication in localized areas, particularly in urban and high-speed scenarios, LEO satellites provide exten-

K.-T. Feng acknowledges support in part by the National Science and Technology Council (NSTC) under Grants NSTC 114-2218-E-A49-019, 113-2221-E-A49-119-MY3, 114-2218-E-A49-017, 112UC2N006, and 112UA10019; in part by the Higher Education Sprout Project of National Yang Ming Chiao Tung University (NYCU) and the Ministry of Education (MoE); in part by the National Defense Science and Technology Academic Collaborative Research Project; in part by the Co-creation Platform of the Industry-Academia Innovation School, NYCU, under the framework of the National Key Fields Industry-University Cooperation and Skilled Personnel Training Act, funded by the MoE and industry partners in Taiwan; in part by Realtek Semiconductor Corp.; and in part by Hon Hai Research Institute. L.-H. Shen acknowledges support by the NSTC under Grant NSTC 113-2222-E-008-008-MY2. Z. Ding acknowledges support by the National Science Foundation under Grant No. 2332760. (Corresponding Author: Kai-Ten Feng)

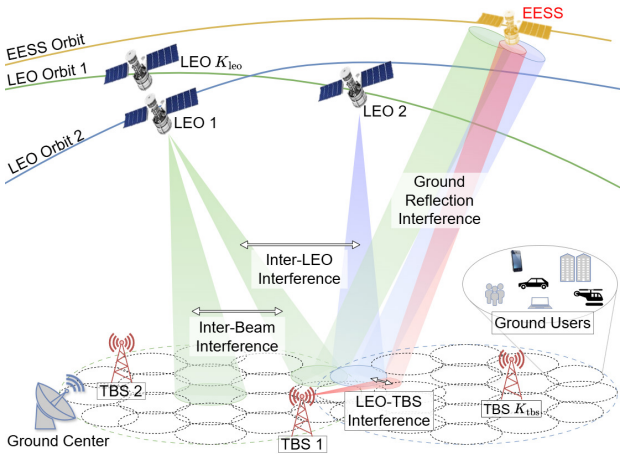

Fig. 1: System architecture of proposed EESS-aware communication system. Ground reflection interference to EESS is considered.

sive global coverage and can serve remote regions with minimal ground infrastructure. By integrating the wide coverage of LEO satellites with the high-capacity capabilities of TBS, communication networks can achieve improved performance, flexibility, and scalability, addressing both localized and global connectivity needs.

However, these studies overlook the challenges of coexistence between communication networks and EESS sensors, which require strict interference regulations to maintain sensing accuracy. This gap highlights the need for novel frameworks that can simultaneously optimize communication network performance while mitigating interference to EESS sensors, thereby enabling their harmonious coexistence. To address the aforementioned challenges, this paper proposes a dynamic resource allocation framework that intelligently balances the requirements of both communication networks and EESS passive sensors. The contribution of this paper are as follows.

- We propose a EESS-aware resource allocation (EARA) scheme that optimizes power allocation, user association, and channel allocation for LEO-TBS system. Additionally, We consider reflected signal interference by model it as a reflected area, considering the worst-case scenario to ensure a conservative interference estimation.
- A non-convex joint optimization problem is formulated to maximize the system data rate while adhering to interference threshold for EESS sensors. By leveraging the Lagrangian dual transform and Dinkelbach's method, the proposed EARA approach efficiently solves the problem under complex constraints.
- Simulation results demonstrate the effectiveness of the EARA scheme in balancing user demands while meeting EESS interference thresholds. We evaluate the EARA scheme under varying user densities to better simulate real-world conditions. Compared to GA and BWOA, the EARA scheme achieves up to a 26.3% improvement in overall system performance.

II. System Model and Problem Formulation

A. System Model

As demonstrated in Fig. 1, we consider a LEO-TBS cooperative communication network under EESS remote sensing tasks. The system employs OFDM to enhance spectral efficiency and minimize interference. It consists of K_{leo} LEOs, denoted by the set $\mathcal{K}_{\text{leo}} = \{1, ..., k, ..., K_{\text{leo}}\}$, and K_{tbs} TBSs, denoted by $\mathcal{K}_{\text{tbs}} = \{1, ..., k, ..., K_{\text{tbs}}\}$. These LEOs and TBSs serve a set of U randomly distributed users, denoted as $\mathcal{U} = \{1, ..., u, ..., U\}$. We consider J_{leo} and J_{tbs} as the number of the beam cells of each LEO and TBS with the respective set indexed by $\mathcal{J}_{\text{leo}} = \{1, ..., j, ..., J_{\text{leo}}\}$ and $\mathcal{J}_{\text{tbs}} = \{1, ..., j, ..., J_{\text{tbs}}\}$. Both LEOs and TBSs share an identical number of sub-channels S, utilizing OFDM. The system bandwidth, denoted by W, is divided into S sub-channels, each sub-channel s with a bandwidth of $W_s = W/S$. For the EESS satellite, we denote h_{eess} as its orbit altitude. As the satellite's sensor scans the area, its sensitivity deteriorates due to harmful interference caused by ground-reflected transmission signal from the LEO-TBS cooperated network. The detailed analysis will be elaborated later.

B. Dynamic User Association Variables

We assume that each user can be served by either a LEO satellite or a TBS, but not both simultaneously. To represent this, we define a binary variable $a^{\chi}_{k,j,u,s}$, which is set to 1 if user u is served by the k-th LEO or TBS in cell j using sub-channel s, and 0 otherwise. The superscript variable $\chi \in \mathcal{V} = \{\text{leo}, \text{tbs}\}$ indicates whether the system is LEO ($\chi = \text{leo}$) or TBS ($\chi = \text{tbs}$). These variables form the set $\mathbf{a} = \{a^{\chi}_{k,j,u,s} \mid \forall \chi, k, j, u, s\}$, which enables dynamic resource allocation and helps to minimize interference between users.

To enforce that each user is exclusively served by either a single LEO or a single TBS, we introduce the following constraint as

$$\sum_{\chi \in \mathcal{V}} \sum_{k \in \mathcal{K}_{\chi}} \sum_{j \in \mathcal{J}_{\chi}} \sum_{s \in \mathcal{S}} a^{\chi}_{k,j,u,s} \leq 1, \quad \forall \chi, u, \tag{1}$$

C. Communication Model

The beamforming gain for each LEO is defined as [11]

$$G_{\text{leo}}(\theta) = G_0 \left[\frac{J_1(\mu(\theta))}{2\mu(\theta)} + 36 \frac{J_3(\mu(\theta))}{\mu(\theta)^3} \right]^2, \tag{2}$$

where θ is the angle measured from the boresight, and G_0 denotes the maximum beamforming gain. $J_1(\cdot)$ and $J_3(\cdot)$ are the Bessel functions of the first and third kinds, respectively, and $\mu(\theta) = 2.01723 \cdot \sin(\theta)/\sin(\theta_{\text{leo}})$, where θ_{leo} is the 3-dB angle. For TBS beamforming gains, the mainlobe and sidelobe beam gains are given by [12]

$$G_{\text{tbs}}(\theta) = \begin{cases} \dfrac{2\pi - (2\pi - \theta)\varepsilon}{\theta_{\text{tbs}}}, & \text{if } \theta \leq \frac{\theta_{\text{tbs}}}{2}, \\ \varepsilon, & \text{otherwise.} \end{cases} \tag{3}$$

Note that the angle measured from the boresight of the TBS beam is denoted as θ and θ_{tbs} represents the mainlobe beamwidth. The parameter $0 < \epsilon \ll 1$ depends on the antenna hardware design. We define the set of power allocations denoted as $\mathbf{P} = \{P^{\chi}_{k,j,s} \mid \forall \chi, k, j, s\}$, where power is allocated to sub-channel s of beam j from either LEO or TBS k. The received signal strength of the ground user u served by beam j on sub-channel s from either LEO or TBS k can be expressed by

$$Y^{\chi}_{n} = P^{\chi}_{k,j,s} G_{\chi}(\theta^{\chi}_{k,j,u}) G^{\text{R}}_{u} H^{\chi}_{k,j,u,s} a^{\chi}_{k,j,u,s}, \tag{4}$$

where $n = (k, j, u, s)$ denotes the tuples of indices and G_u^{R} is the receiver antenna gain and $H_{k,j,u,s}^{\chi} = 10^{-L_{k,j,u,s}^{\chi}/10}$ represents the channel gain from LEO or TBS k. Note that $L_{k,j,u,s}^{\mathrm{leo}} = FL_{k,j,u,s}^{\mathrm{leo}} + AL_{k,j,u,s}^{\mathrm{leo}} + SL_{k,j,u,s}^{\mathrm{leo}}$ denotes the total path loss from LEO in dB [10], including free-space path loss $FL_{k,j,u,s}^{\mathrm{leo}}$, gas absorption loss $AL_{k,j,u,s}^{\mathrm{leo}}$, and tropospheric scintillation loss $SL_{k,j,u,s}^{\mathrm{leo}}$. Similarly, the total path loss from TBS in dB is $L_{k,j,u,s}^{\mathrm{tbs}} = FL_{k,j,u,s}^{\mathrm{tbs}}$. For a user u served by LEO or TBS k, the interference from other beams of LEOs and TBSs is given by

$$\begin{aligned} I_n^{\chi} = &\sum_{j=1}^{J_{\chi}} \sum_{u'=1}^{U} P_{k,j,s}^{\chi} G_{\chi}\left(\theta_{k,j,u}^{\chi}\right) G_u^{\mathrm{R}} H_{k,j,u,s}^{\chi} a_{k,j,u',s}^{\chi} \\ &+ \sum_{k \neq k}^{K_{\chi}} \sum_{j=1}^{J_{\chi}} \sum_{u'=1}^{U} P_{k,j,s}^{\chi} G_{\chi}\left(\theta_{k,j,u}^{\chi}\right) G_u^{\mathrm{R}} H_{k,j,u,s}^{\chi} a_{k,j,u',s}^{\chi} \\ &+ \sum_{k=1}^{K_{\chi'}} \sum_{j=1}^{J_{\chi'}} \sum_{u' \neq u}^{U} P_{k,j,s}^{\chi'} G_{\chi'}\left(\theta_{k,j,u}^{\chi'}\right) G_u^{\mathrm{R}} H_{k,j,u,s}^{\chi'} a_{k,j,u',s}^{\chi'}, \end{aligned} \tag{5}$$

where the tuple $(\chi, \chi') \in \{(\mathrm{leo}, \mathrm{tbs}), (\mathrm{tbs}, \mathrm{leo})\}$. Therefore, we can acquire the signal-to-interference-plus-noise-ratio (SINR) of user u served by beam j on sub-channel s from the k-th LEO or TBS as

$$\Gamma_n^{\chi} = \frac{Y_n^{\chi}}{I_n^{\chi} + \sigma^2}, \tag{6}$$

where $\sigma^2 = N_0 W_s$ represents sub-channel white noise power. The total achievable rate for all downlink (DL) users in the system is

$$R_{\mathrm{tot}} = \sum_{\chi \in \mathcal{V}} \sum_{n \in \Omega_{\chi}} W_s \log_2(1 + \Gamma_n^{\chi}), \tag{7}$$

where $\Omega_{\chi} = \mathcal{K}_{\chi} \times \mathcal{J}_{\chi} \times \mathcal{U} \times \mathcal{S}, \forall \chi$ is the Cartesian product of parameter spaces.

D. EESS Model

We consider a currently operating weather satellite in low Earth orbit at an altitude of approximately 835 km, equipped with a passive microwave sensor F6 [13]. However, if the sensor's orientation is directed toward regions with active communication, it may experience unavoidable interference. To assess this impact, we model the interference received by the EESS sensor, which requires capturing the real antenna pattern of the passive sensor [14]

$$G_{\mathrm{eess}}(\psi) = \begin{cases} G_{\max} - 1.8 \times 10^{-3} \left(\frac{D}{\lambda}\psi\right)^2, & (0^{\mathrm{o}} \leq \psi \leq \psi_{\mathrm{m}}) \\ \max\left(G_{\max} - 1.8 \times 10^{-3} \left(\frac{D}{\lambda}\psi\right)^2, \right. & \\ \left. -5\log\left(\frac{D}{\lambda}\right) - 25\log\left(\psi\right)\right), & (\psi_{\mathrm{m}} < \psi \leq 69^{\mathrm{o}}) \\ -13 - 5\log\left(\frac{D}{\lambda}\right), & (69^{\mathrm{o}} < \psi \leq 180^{\mathrm{o}}), \end{cases} \tag{8}$$

where ψ is the off-axis angle measured from the boresight, ψ_{m} is the 3-dB beamwidth, D is the sensor antenna aperture, λ is the wavelength, and $G_{\max}$ is the maximum beam gain. Different from existing works, we consider the impact of the interference on EESS due to the beam reflection area on the ground, which is not perfectly circular. Accurately computing the interference area is complex. Therefore, we assume a worst-case interference scenario, where the calculated area is slightly larger than the actual reflection area to provide a conservative estimate of the interference impact. The receive interference of the EESS passive sensor is formulated as [6]

$$I_{\mathrm{eess}} = \sum_{\chi \in \mathcal{V}} \sum_{k \in \mathcal{K}_{\chi}} \sum_{j \in \mathcal{J}_{\chi}} \sum_{s \in \mathcal{S}} P_{k,j,s}^{\chi} G_{\mathrm{eess}}(\psi_{k,j}^{\chi}) H_{k,j}^{\prime\chi} A_{k,j}^{\chi}, \tag{9}$$

where $\psi_{k,j}^{\chi}$ denotes the angles between the ground reflection points from beam j of LEO or TBS k and the boresight of the EESS beam. $H_{k,j}^{\prime\chi} = 10^{-L_{k,j}^{\prime\chi}/10}$ represents the channel gains of the reflection links for LEO or TBS beams, where $L_{k,j}^{\prime\chi} = FL_{k,j}^{\chi} + AL_{k,j}^{\chi} + SL_{k,j}^{\chi} + RL$ denotes the total path loss of the reflection link in dB. Note that $FL_{k,j}^{\prime\chi}$ represents the total free-space path loss of the reflection link from LEO or TBS. RL denotes the ground reflection loss, which is assumed to be 4.7 dB [6]. The amplification factors $A_{k,j}^{\chi}$ in (9) capture the interference caused by the reflection areas $Z_{k,j}^{\chi}$, which are the regions illuminated by beam j of the k-th LEO or TBS:

$$A_{k,j}^{\chi} = \iint_{Z_{k,j}^{\chi}} G_{\chi}\left(\phi_{k,j}^{\chi}(\mathbf{z})\right) d\mathbf{z} \approx \int_0^{R_{k,j}^{\chi}} G_{\chi}\left(\theta_{k,j}^{\prime\chi}(r)\right) 2\pi r \, dr, \tag{10}$$

where $\phi_{k,j}^{\chi}(\mathbf{z})$ represents the angles between ground position $\mathbf{z}$ and the boresight direction of EESS sensor from LEO or TBS k's beam j. The reflection areas are approximated as circles, where their radii are defined as $R_{k,n}^{\chi} = h_{k,j}^{\chi} \tan(\theta_{\chi})$. The terms $\theta_{k,j}^{\prime\chi}(r) = \tan^{-1}(r/h_{k,j}^{\chi})$ describes the angles between the beam boresight and a point at distance r within the beam footprint. These approximations simplify the computation of $A_{k,j}^{\chi}$ for practical application while maintaining accuracy in interference estimation.

E. Problem Formulation

Our objective is to maximize the system data rate while ensuring that the interference to the EESS passive sensor remains within acceptable limits. This is achieved by optimizing user association and power allocation of LEOs and TBSs. The optimization problem can be formulated as

$$\max_{\mathbf{a},\mathbf{P}} \quad R_{\mathrm{tot}} \tag{11a}$$

$$\text{s.t.} \quad (1), \tag{11b}$$

$$I_{\mathrm{eess}} \leq \eta_{\mathrm{ITU}}, \tag{11c}$$

$$0 \leq \sum_{j \in \mathcal{J}_{\mathrm{leo}}} \sum_{s \in \mathcal{S}} P_{k,j,s}^{\mathrm{leo}} \leq P_{\max}^{\mathrm{leo}}, \qquad \forall k \in \mathcal{K}_{\mathrm{leo}}, \tag{11d}$$

$$0 \leq \sum_{s \in \mathcal{S}} P_{k,j,s}^{\mathrm{leo}} \leq P_{\mathrm{beam}}^{\mathrm{leo}}, \forall k \in \mathcal{K}_{\mathrm{leo}}, \forall j \in \mathcal{J}_{\mathrm{leo}}, \tag{11e}$$

$$0 \leq \sum_{j \in \mathcal{J}_{\mathrm{tbs}}} \sum_{s \in \mathcal{S}} P_{k,j,s}^{\mathrm{tbs}} \leq P_{\max}^{\mathrm{tbs}}, \qquad \forall k \in \mathcal{K}_{\mathrm{tbs}}, \tag{11f}$$

$$0 \leq \sum_{s \in \mathcal{S}} P_{k,j,s}^{\mathrm{tbs}} \leq P_{\mathrm{beam}}^{\mathrm{tbs}}, \ \forall k \in \mathcal{K}_{\mathrm{tbs}}, \forall j \in \mathcal{J}_{\mathrm{tbs}}, \tag{11g}$$

where constraint (11b) ensures that each user can only be served by either one LEO or one TBS, constraint (11c) ensures that the EESS interference remains below η_{ITU} [13], and (11d) and (11e) respectively constrain the total transmit power for LEO must not exceed $P_{\max}^{\mathrm{leo}}$ and the power allocated to each LEO beam is limited by $P_{\mathrm{beam}}^{\mathrm{leo}}$. Similarly, for TBS, the maximum total transmit power is constrained by $P_{\max}^{\mathrm{tbs}}$, and

the power budget per beam is limited to $P_{\text{beam}}^{\text{tbs}}$, as given in (11f) and (11g), respectively. We observe that problem (11) is non-convex and nonlinear due to the presence of fractional terms. Additionally, the optimization of coupled continuous and discrete variables further increases the complexity of the original problem. Therefore, we propose an effective solution to address this issue, which will be discussed in the following section.

III. Proposed EESS-Aware Resource Allocation (EARA) Scheme

We observed that the objective function of (11) is a summation of logarithmic terms, each contains a fractional SINR. To solve this, we apply the Lagrangian dual transform [15] and Dinkelbach method [16]. Firstly, the constraint (11c) is convex due to the linear relationship between I_{eess} and power allocation variables $P_{k,j}^{\chi}$. The approximated terms $A_{k,j}^{\chi}$ in (9) are precomputed based on the geographical positions and beam patterns of LEO and TBS systems. Based on Lagrange dual transform, we can convert (11a) to a sum-of-ratio form. The new objective function F is formulated as

$$F=\sum_{\chi\in\mathcal{V}}\sum_{n\in\Omega_\chi}\left(\frac{(1+\Gamma_n^\chi)\,Y_n^\chi}{Y_n^\chi+I_n^\chi+\sigma^2}+\log_2(1+\Gamma_n^\chi)-\Gamma_n^\chi\right), \quad (12)$$

where $\mathbf{\Gamma}=\{\Gamma_n^\chi \mid \forall\chi,n\}$ denotes the set of SINR values. We find that F is a differentiable with respect to Γ_n^χ when $\{\mathbf{a}^\chi,\mathbf{P}^\chi\}$. By solving $\frac{\partial F}{\partial\Gamma_n^\chi}=0$, we can obtain the optimal values $\Gamma_n^{\chi,*}$. By substituting $\Gamma_n^{\chi,*}$ into Γ_n^χ in (12), we can observe that the terms non-fractional terms remain constant. Consequently, we can reformulate F into an iterative objective function as

$$\overline{F}=\sum_{\chi\in\mathcal{V}}\sum_{n\in\Omega_\chi}\frac{(1+\Gamma_n^{\chi,(i-1)})Y_n^\chi}{Y_n^\chi+I_n^\chi+\sigma^2}. \quad (13)$$

In i-iteration, $\Gamma_n^{\chi,(i-1)}$ represents the optimal SINR values, which can be obtained by substituting solution from $(i-1)$-iteration $\{\mathbf{a}^{(i-1)},\mathbf{P}^{(i-1)}\}$. However, the received power and interference terms in (13) contain quadratic bilinear products, making direct optimization difficult. To address this, we apply first-order Taylor expansion for a general bilinear function $w(x,y)=xy$ around reference point (x_0,y_0) as

$$w(x,y)\approx x_0y_0+y(x-x_0)+x(y-y_0). \quad (14)$$

We can utilize (14) to linearize the bilinear terms $P_{k,j,s}^\chi\cdot a_{k,j,u,s}^\chi$ in Y_n^χ and I_n^χ as

$$\begin{aligned}&P_{k,j,s}^\chi\cdot a_{k,j,u,s}^\chi\approx P_{k,j,s}^{\chi,(i-1)}\cdot a_{k,j,u,s}^{\chi,(i-1)}\\&+a_{k,j,u,s}^\chi\cdot(P_{k,j,s}^\chi-P_{k,j,s}^{\chi,(i-1)})+P_{k,j,s}^\chi\cdot(a_{k,j,u,s}^\chi-a_{k,j,u,s}^{\chi,(i-1)}). \quad (15)\end{aligned}$$

Here, the expansion is centered around a reference point $\left(P_{k,j,s}^{\chi,(i-1)},a_{k,j,u,s}^{\chi,(i-1)}\right)$ to iteratively approach a stable convergence point. After substituting these linearized expressions into (4) and (5), the objective function is reformulated as a convex function, and the equivalent optimization problem is expressed as

$$\begin{aligned}\max_{\mathbf{a},\mathbf{P}}\quad&\overline{F}, &(16a)\\ \text{s.t.}\quad&(11b),(11c),(11d),(11e),(11f),(11g). &(16b)\end{aligned}$$

Since the robjective function in (16) still contains fractional terms, it remains non-convex. To address this, we apply Dinkelbach's method [16] to transform the fractional expressions into a sequence of solvable programs:

$$\widetilde{F}=\sum_{\chi\in\mathcal{V}}\sum_{n\in\Omega_\chi}\left((1+\Gamma_n^{\chi,(i-1)})Y_n^\chi-t_n^{\chi,(i-1)}(Y_n^\chi+I_n^\chi+\sigma^2)\right), \quad (17)$$

where the SINR values $\Gamma_n^{\chi,(i-1)}$ are obtained from the previous iteration. Note that $t_n^{\chi,(i-1)}$ represents the optimal Lagrange multipliers in the i-th iteration, which can be calculated as

$$t_n^{\chi,(i-1)}=\frac{(1+\Gamma_n^{\chi,(i-1)})\;Y_n^{\chi,(i-1)}}{Y_n^{\chi,(i-1)}+I_n^{\chi,(i-1)}+\sigma^2}, \quad (18)$$

where $Y_n^{\chi,(i-1)}$ and $I_n^{\chi,(i-1)}$ can be obtained from previous iteration. The updated optimization problem is then formulated as

$$\max_{\mathbf{a},\mathbf{P}}\quad\widetilde{F}\qquad\text{s.t.}\quad(16b). \quad (19)$$

The current problem is still non-convex due to the binary user association variable $a_{k,j,u,s}^\chi$. Motivated by [17], to solve binary variable problem, we relax the user association variable between 0 and 1, and formulate an additional constraints as

$$0\le\;a_{k,j,u,s}^\chi\le 1,\forall\chi,k,j,u,s. \quad (20)$$

To enforce the relaxed variables to remain close to 0 or 1, we transform the relaxed terms into penalty functions, which are denoted as $G_\chi(\mathbf{a})=\sum_{\chi\in\mathcal{V}}\sum_{n\in\Omega_\chi}a_n^\chi(1-a_n^\chi)$. Since $G_\chi(\mathbf{a})$ is quadratic and non-convex, we apply a first-order Taylor approximation to linearize the expression of $G_\chi(\mathbf{a})$ as

$$G'_\chi(\mathbf{a})=G_\chi(\mathbf{a}^{(i-1)})+(\mathbf{a}^{(i)}-\mathbf{a}^{(i-1)})\cdot\nabla_{\mathbf{a}}^TG_\chi(\mathbf{a}^{(i-1)}), \quad (21)$$

where the partial derivatives in (21) are derived as $\frac{\partial G_\chi(\mathbf{a})}{\partial a_{k,j,u,s}}=1-2a_{k,j,u,s}^\chi$ with superscript T indicating the transpose operation. Consequently, we can rewrite our ultimate optimization problem as

$$\begin{aligned}\max_{\mathbf{a},\mathbf{P}}\quad&\widetilde{F}-\beta_{\text{leo}}G'_{\text{leo}}(\mathbf{a})-\beta_{\text{tbs}}G'_{\text{tbs}}(\mathbf{a}) &(22a)\\ \text{s.t.}\quad&(16b),(20), &(22b)\end{aligned}$$

where β_{leo} and β_{tbs} are the penalty factors. The final formulation in (22) results in a convex optimization problem, which we solve using C.V.X. [18]. The complete steps of the proposed EARA scheme are described in Algorithm 1. In practical scenarios, the algorithm can be implemented in a ground control center to manage LEO and TBS. The procedure iterates until the convergence condition $|R_{tot}^{(i)}-R_{tot}^{(i-1)}|\le\rho_R$ is met and the maximum number of iterations $i=I$ is reached, where ρ_R denotes the convergence threshold of data rate and I represents the iteration limit.

IV. Performance Evaluation

We adopt a realistic map of the United States for our simulation and focus on California as the study region. The LEO satellite constellation and movement parameters are based on [11]. TBSs are deployed randomly within the study area. For user distribution, a portion of the total users is placed non-uniformly near the TBSs, while the remaining users are randomly distributed across the area. The system parameters

Algorithm 1: Proposed EARA Scheme

Input: Initial user association set set $\{\mathbf{a}^{(0)}\}$, and power allocation set $\{\mathbf{P}^{(0)}\}$.
Output: Optimized solution set $\{\mathbf{a}, \mathbf{P}\}$ and data rate R_{tot}.
Initialize iteration index $i = 1$ and compute the initial system data rate $R_{\text{tot}}^{(0)}$ using $\{\mathbf{a}^{(0)}, \mathbf{P}^{(0)}\}$.
repeat
    Solve the optimization problem with fixed $\{\mathbf{a}^{(i-1)}, \mathbf{P}^{(i-1)}\}$, and obtain current solution set $\{\mathbf{a}^{(i)}, \mathbf{P}^{(i)}\}$.
    Calculate current data rate $R_{\text{tot}}^{(i)}$.
    if $|R_{\text{tot}}^{(i)} - R_{\text{tot}}^{(i-1)}| \leq \rho_R$ **then**
        Break: Convergence criteria met.
    end if
until iteration index i reaches I.

TABLE I: Setting Parameters

System Parameters	Value
Carrier frequency (f_c)	20 GHz
Total system bandwidth	100 MHz
Number of sub-channel (S)	8
Number of beams in a LEO (M)	7
Altitude of LEO (h_{leo})	550 km
Noise power spectral density (N_0)	-174 dBm/Hz
LEO/beam power budget ($P_{\max}^{\text{leo}}$,$P_{\text{beam}}^{\text{leo}}$)	30, 10 dBW
TBS/beam power budget ($P_{\max}^{\text{tbs}}$,$P_{\text{beam}}^{\text{tbs}}$)	10, -10 dBW
Antenna aperture	$10c/f_c$
EESS interference threshold (η_{ITU}) [13]	-166 dBm
LEO 3dB beamwidth/transmitter gain (θ_{leo},G_0)	0.058 rad, 40 dBi
TBS antenna parameter (ϵ)	0.01
Receiver antenna gain of user (G_u^{r})	40 dBi
Maximum beam gain of EESS sensor ($G_{\max}$) [13]	34.4 dBi
Altitude of EESS (h_{eess})	835 km

are summarized in Table I. We simulate an EESS satellite conducting an Earth observation mission.

The convergence behavior of the proposed EARA scheme is illustrated in Fig. 2(a). We compare two scenarios: one with the EESS interference constraint enforced and the other without, under different TBS density. We can observe that the data rates converge within five iteration. When EESS constraints are enforced, increasing TBS density yields only marginal improvements in data rate. This is because TBS interference contributes more significantly to EESS impacts than LEO interference. As a result, EARA scheme tends to prioritize LEO-based communication over TBS in order to mitigate interference.

Fig. 2(b) illustrates the relationship between TBS density and data rate. Without EESS constraints, increasing TBS density leads to higher data rates due to improved network capacity. Since TBS generally provides better channel conditions than LEO, the algorithm allocates more traffic to TBS to maximize overall performance. However, when EESS constraint are active, the data rate saturates beyond a certain TBS density. This indicates that EESS interference regulations impose significant limitations on the potential benefits of dense network deployments, highlighting the need for adaptive resource allocation strategies to balance communication performance and interference mitigation.

In Fig. 3, we evaluate the impact of EESS interference on data rate performance. The EESS travels along the California coastline, starting near Los Angeles (approximately 34°03' N), passing through the South Bay Area near San Jose (37°20' N), and reaching San Francisco (37°46' N), continuing northwest thereafter. The x-axis in Fig. 3 represents EESS latitude, with the Bay Area at the midpoint, where most user is located. As the EESS approaches the Bay Area, interference increases, causing a significant drop in sum rate. The effect is most severe

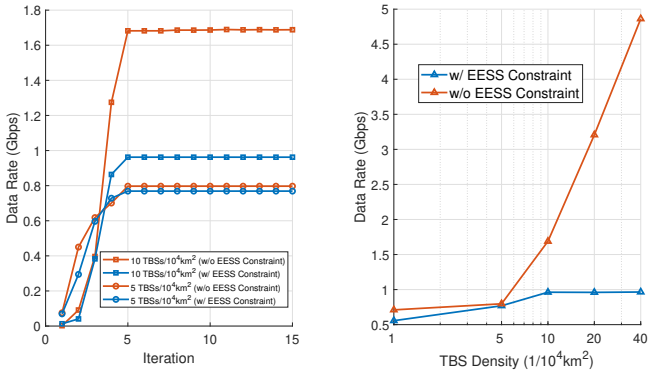

(a) (b)

Fig. 2: Convergence and data rate performance of EARA under different TBS densities with and without EESS constraints. (a) Convergence over iterations for different TBS densities. (b) Relationship between TBS density and achievable data rate.

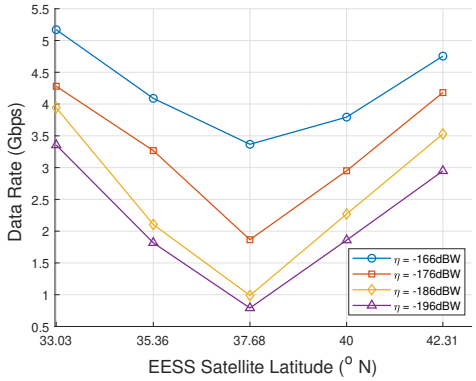

Fig. 3: Data rate performance of EARA under varying EESS satellite latitudes and interference thresholds.

when the EESS is directly overhead. As it moves northwest, the interference decreases, leading to performance recovery. Different curves in Fig. 3 correspond to EESS interference thresholds $\eta = \{-166, -176, -186, -196\}$ dBW. Higher thresholds (i.e., more relaxed constraints) result in better data rates, while tighter thresholds like $\eta = -196$ dBW cause more severe degradation, especially in densely populated regions. These results highlight the trade-off between interference mitigation and communication efficiency, underscoring the need for adaptive resource allocation that accounts for EESS movement.

In Fig. 4, we observe the impact of different LEO and TBS beam power budgets on system data rate under varying population densities. The configurations include LEO beam power settings $P_{\text{beam}}^{\text{leo}} = \{10, 15, 20\}$ dBW and TBS beam power settings $P_{\text{beam}}^{\text{tbs}} = \{-10, 0\}$ dBW. As population density increases, data rate declines due to intensified resource contention and interference, particularly the interference imposed by EESS constraint. Higher LEO beam power enhances data rates, especially in low-density areas, by increasing signal gain. Lower TBS power also enhances performance by reducing interference, particularly in regions with overlapping beams. However, as population density continue to rise, the performance gap between configurations narrows, indicating that interference and resource constraints dominate in highly populated areas.

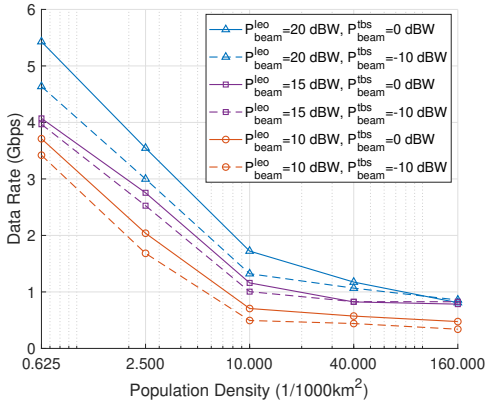

Fig. 4: Data rate performance of EARA under varying population densities and different power allocations budget for LEO and TBS beams.

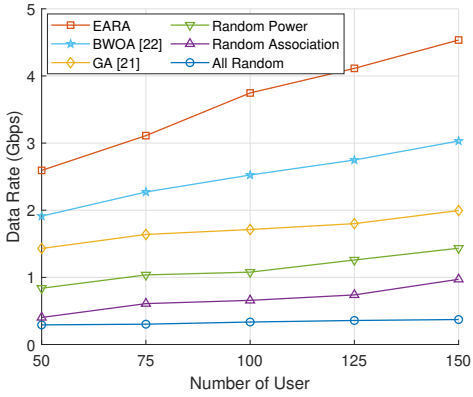

Fig. 5: Performance comparison of EARA with existing benchmarks: data rate versus number of user.

Fig. 5 compares the proposed EARA scheme with two benchmark algorithms and two random allocation strategies, i.e, **Benchmark 1**: the genetic algorithm (GA) [19], and **Benchmark 2**: binary whale optimization Algorithm (BWOA) [20]: **Random Power** optimizes only user association $\mathbf{a}$, **Random Association** optimizes only power allocation $\mathbf{P}$. The EARA scheme consistently achieves the highest sum rate, 26.3% over Benchmark 2. Benchmark 2 outperforms Benchmark 1, demonstrating its advantage in handling mixed-integer optimization problems. However, both benchmarks suffer from scalability issues. As the search space for power allocation and user association expands, they are more prone to local optima and suboptimal performance. Random Power outperforms Random Association, indicating that user association has a greater impact on performance due to its larger and more complex search space. Fully random allocation yields the lowest performance, underscoring the necessity of joint optimization in both user association and power allocation.

V. Conclusion

In this paper, we evaluated how terrestrial communication systems can coexisit with EESS operations by considering the worst-case interference scenario. Our proposed EARA scheme maximizes downlink data rate while ensuring that interference to EESS sensors remains below the ITU-defined threshold. We applied Lagrange's dual transform and Dinkelbach's method to solve the resulting non-convex optimization problem. Simulation results demonstrate the effectiveness of proposed framework in balancing communication performance and interference mitigation. The results highlighted the superiority of the EARA scheme over existing algorithms, including GA and BWOA. Furthermore, the analysis emphasized the critical trade-offs between interference constraints and communication efficiency, especially when the EESS satellite is in close proximity to dense user regions. This work provided a foundation for future research on the harmonious coexistence of next-generation communication networks and Earth observation systems.

References

[1] ITU, *Handbook on Earth Exploration-Satellite Service*. United Nations Fund for Population Activities, 2011.

[2] V. H. Payne, E. J. Mlawer, K. E. Cady-Pereira, and J.-L. Moncet, "Water Vapor Continuum Absorption in the Microwave," *IEEE Trans. Geosci. Remote Sens.*, vol. 49, no. 6, pp. 2194–2208, 2011.

[3] M. Yousefvand, C.-T. M. Wu, R.-Q. Wang, J. Brodie, and N. Mandayam, "Modeling the Impact of 5G Leakage on Weather Prediction," in *Proc. IEEE 5G World Forum (5GWF)*, 2020, pp. 291–296.

[4] M. J. Marcus, "5G/Weather Satellite 24 GHz Spectrum Disagreement: Anatomy of a Spectrum Policy Issue," *IEEE Wireless Commun.*, vol. 26, no. 4, pp. 2–3, 2019.

[5] A. Palade, A. M. Voicu, P. Mähönen, and L. Simić, "Will Emerging Millimeter-Wave Cellular Networks Cause Harmful Interference to Weather Satellites?" *IEEE Trans. on Cognitive Commun. and Networking*, vol. 9, no. 6, pp. 1546–1560, 2023.

[6] P. Testolina, M. Polese, J. M. Jornet, T. Melodia, and M. Zorzi, "Modeling Interference for the Coexistence of 6G Networks and Passive Sensing Systems," *IEEE Trans. Wireless Commun.*, vol. 23, no. 8, pp. 9220–9234, 2024.

[7] M. Polese, V. Ariyarathna, P. Sen, J. Siles, F. Restuccia, T. Melodia, and J. M. Jornet, "Dynamic Spectrum Sharing Between Active and Passive Users Above 100 GHz," *Nature Commun. Eng.*, vol. 1, no. 6, 2022.

[8] S. Li, Z. Dong, Q. Wang, W. Zhou, and W. Xiao, "Resource Allocation for Multiple Base Stations OFDM Systems under High-Speed Scenarios," in *Proc. IEEE Int. Conf. Commun. Technol. (ICCT)*, 2021, pp. 937–941.

[9] D. W. K. Ng, E. S. Lo, and R. Schober, "Energy-Efficient Resource Allocation in OFDMA Systems with Large Numbers of Base Station Antennas," *IEEE Trans. Wireless Commun.*, vol. 11, no. 9, pp. 3292–3304, 2012.

[10] L.-H. Shen, Y. Ho, K.-T. Feng, L.-L. Yang, S.-H. Wu, and J.-M. Wu, "Hierarchical Multi-Agent Multi-Armed Bandit for Resource Allocation in Multi-LEO Satellite Constellation Networks," in *Proc. IEEE Veh. Technol. Conf. (VTC-Spring)*, 2023, pp. 1–5.

[11] S.-H. Chen, L.-H. Shen, K.-T. Feng, L.-L. Yang, and J.-M. Wu, "Energy-Efficient Joint Handover and Beam Switching Scheme for Multi-LEO Networks," in *Proc. IEEE Veh. Technol. Conf. (VTC-Spring)*, 2024, pp. 1–7.

[12] L.-H. Shen and K.-T. Feng, "Mobility-Aware Subband and Beam Resource Allocation Schemes for Millimeter Wave Wireless Networks," *IEEE Trans. Veh. Technol.*, vol. 69, no. 10, pp. 11 893–11 908, 2020.

[13] ITU-R, "Typical technical and operational characteristics of Earth exploration-satellite service (passive) systems using allocations between 1.4 and 275 GHz," RS.1861-1, Dec. 2021.

[14] ——, "Reference antenna pattern for passive sensors operating in the Earth exploration-satellite service (passive) to be used in compatibility analyses in the frequency range 1.4-450 GHz," RS.1813-1, Dec. 2021.

[15] L.-H. Shen, C.-J. Ku, and K.-T. Feng, "Downlink Rate Maximization With Reconfigurable Intelligent Surface Assisted Full-Duplex Transmissions," *IEEE Trans. Veh. Technol.*, vol. 73, no. 8, pp. 12 264–12 269, 2024.

[16] W. Dinkelbach, "On Nonlinear Fractional Programming," *Management Science*, vol. 13, no. 7, pp. 492–498, 1967. [Online]. Available: http://www.jstor.org/stable/2627691

[17] L.-H. Shen, P.-Y. Wu, and K.-T. Feng, "Energy Efficient Resource Allocation for Multinumerology Enabled Hybrid Services in B5G Wireless Mobile Networks," *IEEE Trans. Wireless Commun.*, vol. 22, no. 3, pp. 1712–1729, 2023.

[18] B. R. Marks and G. P. Wright, "A General Inner Approximation Algorithm for Nonconvex Mathematical Programs," *Operations Research*, vol. 26, no. 4, pp. 681–683, 1978. [Online]. Available: http://www.jstor.org/stable/169728

[19] Y.-T. Li, L.-H. Shen, K.-T. Feng, and C.-Y. Chan, "Genetic Multi-Agent Reinforcement Learning for Multiple Double-Sided STAR-RISs in Full-Duplex MIMO Networks," in *Proc. IEEE Int. Conf. Commun. (ICC)*, 2024, pp. 5003–5008.

[20] Q.-V. Pham, S. Mirjalili, N. Kumar, M. Alazab, and W.-J. Hwang, "Whale Optimization Algorithm With Applications to Resource Allocation in Wireless Networks," *IEEE Trans. Veh. Technol.*, vol. 69, no. 4, pp. 4285–4297, 2020.